Received: 16 May 2023 | Accepted: 26 August 2023

DOI: 10.1111/1365-2478.13422

Geophysical Prospecting | EAGE EUROPEAN ASSOCIATION OF GEOSCIENTISTS & ENGINEERS

ORIGINAL ARTICLE

Depth-based correlation analysis between the density of lineaments in the crystalline basement's weathered zones and groundwater occurrences within the Voltaian basin, Ghana

Theophilus Yaw Amponsah[1,2] | **David Dotse Wemegah**[2] | **Sylvester Kojo Danuor**[2] | **Eric Dominic Forson**[3,4]

[1]Council for Scientific and Industrial Research-Institute of Industrial Research, Accra, Ghana

[2]Geophysics Section, Department of Physics, Kwame Nkrumah University of Science and Technology, Kumasi, Ghana

[3]Department of Physics, School of Physical and Mathematical Sciences, University of Ghana, Legon, Accra, Ghana

[4]CODES-ARC Centre of Excellence in Ore Deposits and School of Earth Science, University of Tasmania, Hobart, Tasmania, Australia

Correspondence
Eric Dominic Forson, Department of Physics, School of Physical and Mathematical Sciences, University of Ghana, Legon, Accra, Ghana. Email: ericdforson@gmail.com and edforson@ug.edu.gh

Abstract

Geological structures have been shown by studies to have influence on the occurrence, storage and transportation of groundwater. Understanding the structural network of an area unearths a deep insight into the groundwater dynamics of the area. A geological structural analysis was carried out to reveal the geological structural network of Ghana's Voltaian basin. Using aeromagnetic data, structural density models were generated using the Center for Exploration Targeting grid analysis technique for two depth ranges (that is up to 100 m and 300 m) over the Voltaian basin. The total length of geological structures (lineaments) delineated at depths up to 100 m and 300 m were more than 5000 km and more than 8000 km, respectively. Given this, the study area was observed to be structurally dense at each of the aforementioned depths. The structural density models were discretized into five classes (very low, low, moderate, moderately high and very high regions), each of which was evaluated to determine their spatial association with known locations of groundwater occurrences within the study area using the frequency ratio technique. Frequency ratio results for both structural density models derived at 100 m and 300 m depths show the existence of a strong correlation between high structural density model classes and the known groundwater occurrences. The structural density models were further evaluated using the receiver operating characteristics curve. The area under the receiver operating characteristics curve scores indicates that, although both structural density models showed very good performance (with receiver operating characteristics scores greater than 0.7), the 300-m depth structural density model performed better than the structural density model generated at a depth of 100 m (with their receiver operating characteristics scores being 0.721 and 0.715, respectively). The obtained results corroborate with literature assertion that groundwater occurrence within the Voltaian basin is mainly associated with structural features. It is expected that the outputs of this study would guide future groundwater exploration programmes within the study area.

KEYWORDS

aeromagnetic data, frequency ratio, groundwater occurrence, lineaments, receiver operating characteristics, structural density model, Voltaian basin

INTRODUCTION

Surface water resources within the Voltaian basin are largely ephemeral owing to the several climatic conditions over the region. The vulnerability of surface water resources to climatic variability explains the seasonal variations, which result in water scarcity at certain periods of the year. The climate-induced scarcity coupled with the continuous destruction of surface water resources has significantly resulted in an increasing demand for groundwater as a potable water resource in many households and firms. This is very evident in the northern sector of Ghana where most surface water resources are largely ephemeral due to harsh weather conditions (Mul et al., 2015). Groundwater accounts for about 60% of the freshwater supplies in the Voltaian basin (Obuobie et al., 2016). Groundwater in a normal basement terrain is found in weathered and fractured aquifers as well as in the transition region (partly weathered basement) between the weathered rock and the fresh bedrock (MacDonald et al., 2011). In contrast to other sedimentary formations, aquifer lengths and depth extents differ greatly in the Voltaian basin (Mainoo et al., 2019). Groundwater availability within the Voltaian basin is mainly due to secondary porosity, thus groundwater within the basin is strongly dependent on fractures and folds (Mul et al., 2015).

Fractures and folds are important structural characteristics that influence groundwater. Fractures are created by the brittle breaking of rocks and are classified as joints, fissures and faults (Roberts, 1982). Folds are formed by ductile deformation, and the magnitude of the features formed, including synclines and anticlines, is determined by the degree of this deformation. Fractures function as hydrodynamic conduits and hence are essential pathfinders to groundwater aquifer's flow pattern. They could serve as hydraulic conductors or as flow barriers in shallow and deep flow. In geological terranes such as the Voltaian basin, where primary porosity and permeability are absent owing to cementation and sedimentation, the occurrence of structures is the most important feature that facilitates groundwater recharge and flow in the subsurface (Mul et al., 2015). The detection of various zones of geological structure occurrence, which also include fault zones, fold hinges and joints are essential components that guide the selection of target areas for groundwater extraction. In view of this, Sankar (2002) suggested that sites of boreholes should be selected with careful consideration of the lithological and structural environment. While the significance of geological structures (lineaments) is widely acknowledged, further studies are needed to fully comprehend the function and behaviour of these features. Thus, areas with high structural density can have significant groundwater prospects even in hilly regions. Geological structural network mapping is regarded as a critical method used in detecting hot springs and conducting hydrogeological research (Sabins, 1999). Its enormous contribution to groundwater dynamics in the subsurface implies fractures are essential factors for groundwater targeting and efficient exploration. Hydro-geophysical analysis, particularly in groundwater development related issues, often includes aquifer potential evaluation, water quality and contamination assessment as well as aquifer vulnerability/protective capability analysis, among other things (Kinnear et al., 2013; Nwachukwu et al., 2018).

In Ghana, vulnerability to drought are influenced by geographical patterns and affects socioeconomic conditions. According to national and regional vulnerability evaluations, the northern regions are the most vulnerable regions to drought in Ghana. Also, these regions have the lowest adaptation capability in the country due to poor socioeconomic development and over-reliance on rain-fed systems like agriculture and forestry for local economies and livelihoods. Climate change is negatively affecting rural livelihoods in these places, as yearly rainfall is decreasing and rainfall patterns are becoming more variable. Extreme weather events, drought and flooding are posing increasing problems to communities. Although water is a vital thematic objective in Ghana's development agenda, it is yet becoming increasingly scarce in northern Ghana due to climate change (Alhassan & Hadwen, 2017). The study of the structural complexity is hinged on the premise that groundwater accumulation, flow and storage are largely dependent on the geological structures in the Voltaian basin (Mul et al., 2015). This is reported to be the case because groundwater in the Voltaian basin mainly occurs and flows in fracture zones and along bedding planes for some areas due to the fact that the primary porosity of these rocks is destroyed through consolidation and cementation (Loh et al., 2020). Structural complexity delineation therefore provides insight into groundwater availability and accessibility (Yidana, 2010). A critical part of the structural complexity analysis is the depth at which these structures occur as this provides information about the accessibility of groundwater in the area as well as the operational depth for groundwater explorers. The method of exploration is thereafter based on this premise. The occurrence of deep-seated water-bearing structures implies that groundwater sources in the area are deep seated, and hence groundwater exploration methods capable of probing deeper must be employed to reach these depths. However, if the structures are found to be within the near subsurface (thus structures are shallow seated), then a shallow groundwater exploration technique must be employed (Kinnear et al., 2013; Nwachukwu et al., 2018). It is also worth noting that the assessment of structural density (structural occurrence) at deeper depths and their relationship with groundwater over the Voltaian basin has been rarely studied. Thus, this study seeks to complement efforts in groundwater research in the Voltaian basin by assessing the relationship between the groundwater potential of the various geological structural networks of the area using the frequency ratio and

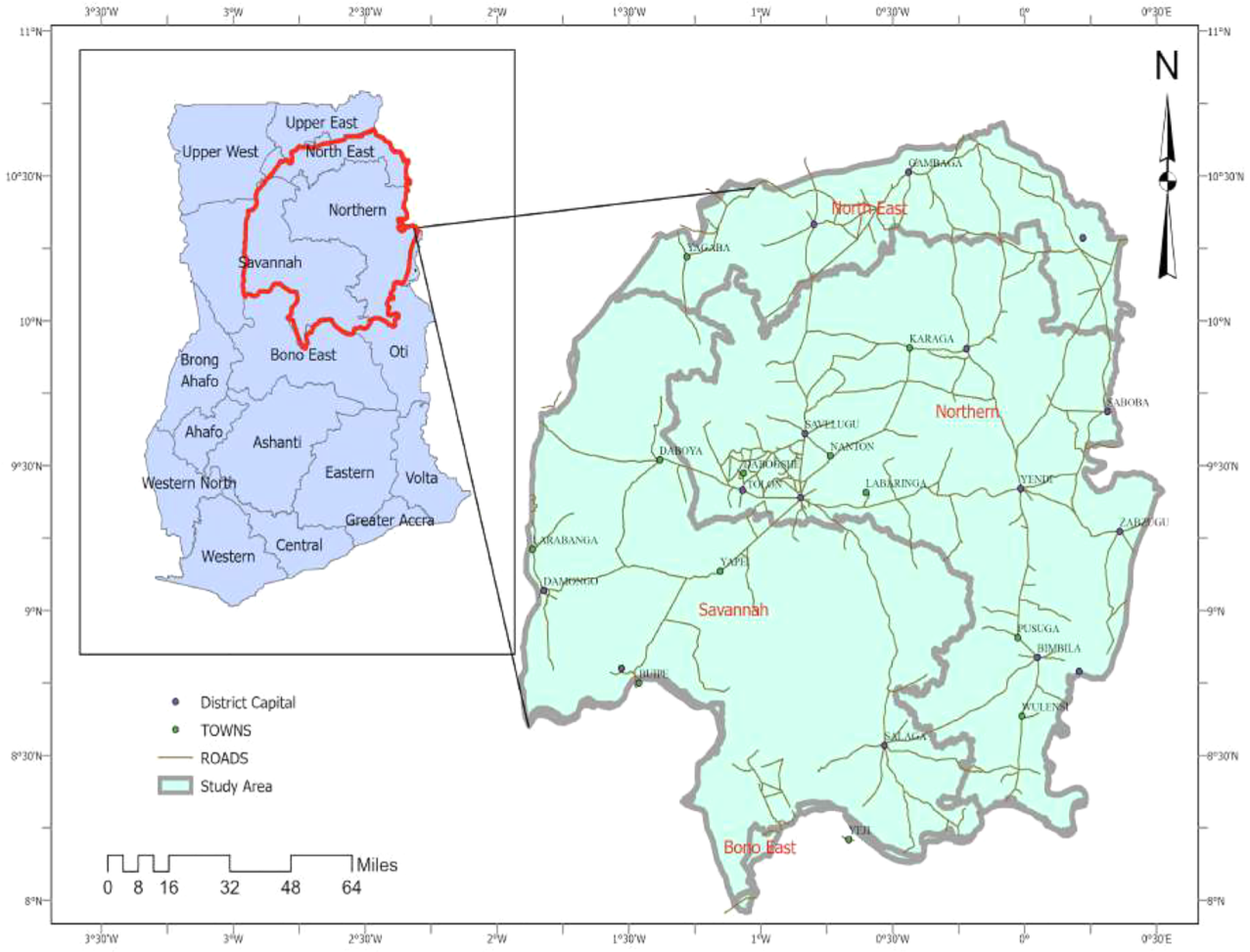

FIGURE 1 A map showing various administrative regions within the study area.

the receiver operating characteristics techniques. It would also provide information on the depth of occurrence of geological structures in the region as well as their spatial correlation with groundwater occurrence within the region. The findings of this research would help in efforts aimed at making water available and accessible. This would provide the needed boost in the socio-economics of the area and would subsequently push the region a step further in the pursuit of poverty alleviation and accessibility to potable water as envisaged in the United Nations Sustainable Development Goals 1 and 6 (SDG1 and SDG6).

STUDY AREA

Location and climate

The study area is located within latitudes 0.369° E and 1.971° W and longitudes 10.788° N and 8.469° N in the northern part of Ghana (Service, 2014). It covers a total land surface area of about 44,558.6 km^2, making up about half of the entire Voltaian basin, as shown in Figure. 1, which has also been known to occupy about one-third of the total land surface area of Ghana. The study area covers areas in the Northern region and some significant parts of the Upper East, Brong Ahafo, Savannah and Oti regions of Ghana. Some major towns within the study area include Pusiga, Daboya, Buipe, Tolon, Savelegu, Dabogshe, Nyampala, Tong, Damango, Yapei, Yendi and Bimbila among others.

Geology and hydrogeology of the Voltaian basin

The area within which this study is undertaken (Figure 1) covers the northern portion of the Voltaian basin, which has been classified into three major lithostratigraphic schemes (Figure 2) (Carney et al., 2010). The Voltaian basin is primarily composed of sediments that lie flat or gradually dip and sit uncomformably on the predominant Precambrian system (Griffis et al., 2002). The unconformities are caused by the high rate of erosion that spans a considerable portion of the basin (Griffis et al., 2002). It is a heterogeneous basin that

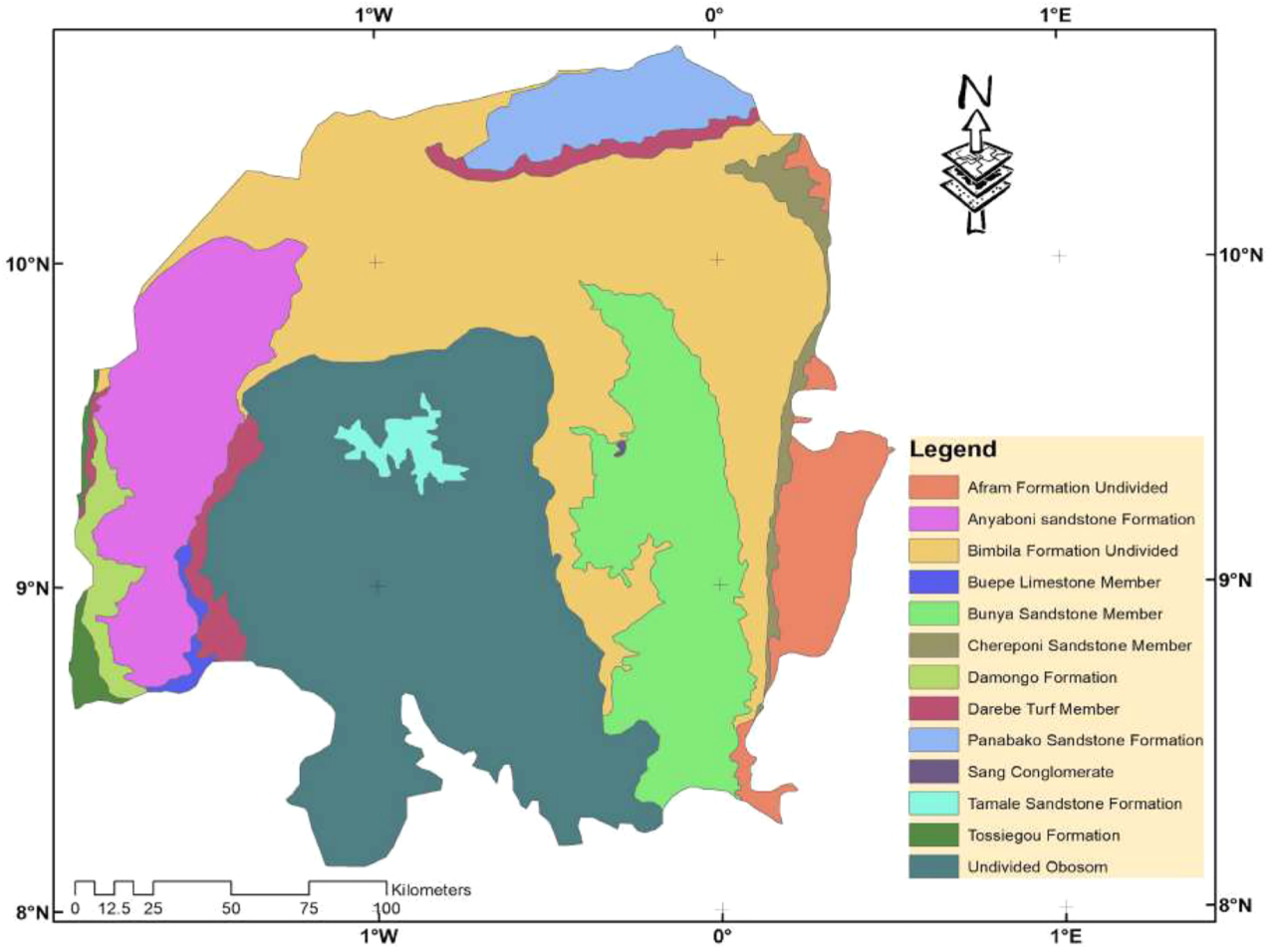

FIGURE 2 Geological map of the study area (modified after GSD, 2010.).

is primarily made up of limestone, mudstones, shale, sandstones and sandy and pebbly beds. This basin's inferred age and correlation are related to the Neoproterozoic and Late Meso-Proterozoic epochs (Jordan et al., 2009). Lithostratigraphically, the Voltaian basin is classified into the Obosum Group, Oti-Pendjari Group and Kwahu Group, which are generally referred to as the Upper Voltaian, Middle Voltaian, and Lower Voltaian, respectively, in the old literature (Annan-Yorke & Cudjoe, 1971). The study area is underlain by rocks from the Sang Conglomerate, Tamale Sandstone Formation and undivided Obosom Formation (Obosom Group) as well as Afram Formation, Bimbilla Formation, Buipe Limestone Member, Bunya Formation, Chereponi Sandstone Member and Darebe Tuff Member of the Oti-Pendjari Group. The area also features the Kwahu Group constituted by the Anyaboni Sandstone Formation, Damongo Formation, Panabako Sandstone Formation and Tossiegou Formation (as shown in Figure 2) (Jordan et al., 2009). Except in a few places, the Voltaian rocks are mainly flat and impermeable. There may be exceptions in locations where due to weathering porous and permeable surface materials have formed from jointed sandstones, arkoses and quartzite. Because the rock lacks primary porosity, hydrogeological conditions are determined by the existence and intensity of weathering and fracturing (Yidana et al., 2019). The Voltaian basin has a fairly limited groundwater capacity in general, though some water does come from fractures in the clay or loose portions of the arenaceous group (Chegbeleh et al., 2009). Regional hydrogeology surveys have revealed that cracks or joints are irregular in some regions and frequently absent. The hydrogeology of the area has been well explained by T. Y. Amponsah et al. (2022). This shows that the capacity of groundwater in the region is complex and demands rigorous research strategies to unravel its prospects and dynamics. The majority of groundwater found in this terrane is hosted in semi-confined and confined aquifers. A good number of hydrogeologists, such as Kortatsi (1994), have documented that the yield potential is generally poor in Voltaian rocks. The hydraulic characteristics of the Voltaian sedimentary environment were also characterized as heterogeneous with the moderate-to-low transmissivity values ranging extensively from 0.2 to 267 m^2 per day in the clay-rich Obosum shale and mudstone environment (Dzigbodi-Adjimah, 1993). Available data reveal that the mean depth of boreholes for most areas is around 90 m and the average depth is 48.1 m

TABLE 1 Survey parameters and specifications for the airborne magnetic survey (Jordan et al., 2009).

Survey parameter	Specification used
Minimum line length	1200 m
Flight line spacing	500 m
Trend of the flight line	135˚
Tie line spacing	5000 m
Trend of the tie line	225˚
Nominal terrain clearance	75 m
Data sampling time	0.05 s

(Yidana et al., 2019). However, in the far-eastern part of the system, there is a record of just a few boreholes above 100 m, even to around 150 m. The weathered or loosened areas range from 4 to 20 m in some parts of the south side of the Voltaian basin, and inhabitants rely on the hand-dug boreholes for their water supplies (Chegbeleh et al., 2009). Boreholes yield values ranging between 5 and 1200 L/min, the amount of static water is 1–20 m, and the fluctuations in the water table average about 4 m (Acheampong & Hess, 1998). Transmissivities are measured between 0.3 and 270 m^2/day (Darko & Krásny, 2007). Groundwater recharge depends on the surface infiltration and permeability of the nearby geological material that shields the aquifer from one location to another. The available literature shows that the annual precipitation within the Voltaian basin ranges between 3.7% and 5% (Apambire, 2000; Martin & Van De Giesen, 2005). The annual groundwater extraction is estimated at less than 5% (Martin & Van De Giesen, 2005).

METHODS

Data

The main data used in this study were sourced from an airborne magnetic survey that was carried out in 2008 over the entire Keta and Volta basins in Ghana by Fugro Airborne Surveys of Perth under the Mining Sector Support Program of the Government of Ghana and supervised by the Ghana Geological Survey Authority (GSD, 2010; Jordan et al., 2009). The magnetic data were processed and analysed further to increase their quality and render them more applicable to the research objectives. The data was taken through various stages of enhancement to improve its quality. This made it easier to delineate fault, fracture and contact features that may regulate groundwater dynamics such as accumulation and flow in the study area (Reeves, 1989). The survey parameters and specifications employed during the airborne magnetic survey are summarized in Table 1.

Data processing

The magnetic method has progressed from its initial use as a tool for finding iron ore to a common tool for mineral, hydrocarbon, groundwater and geothermal resource exploration. The technique is often widely used in other applications, such as water-resource assessment studies and determining the best location for water deposition based on the depth of the basement and other related geological structures. It is also used to assess the thickness of surface alluvial sediments and their basins (Blakely et al., 1973; Smith et al., 2004). In this study, the use of aeromagnetic data played a primal role in the delineation of various geological structures (lineaments) as well as their densities over the study area. This was preceded by applying the reduction-to-equator (RTE) technique to the residual magnetic intensity (shown in Figure 3) and subsequently inverting it to generate magnetic responses that are symmetrical to their respective sources, which is denoted as RTE_Inv. Afterwards, the first vertical derivative as an edge detection method was employed on the RTE_Inv to delineate various structures within the study area. The upward continuation and downward continuation (DC) filtering techniques were, respectively, applied on the RTE_Inv grid to further transform and visualize the magnetic intensity responses at different depths below the surface of the Earth. In the case of the upward continuation, it was carried out on the RTE_Inv to suppress shallow anomalies hence enhancing deep-seated anomalies at a depth of 300 m. Thus, the upward continuation (UC) operation filter aided the transformation of the potential field (aeromagnetic) data measured on one surface to a higher surface (Nabighian et al., 2005). The use of the UC filter was plausible because it preserves primarily longer wavelengths at higher observation levels, whereas short-wavelength anomalies caused by small-sized near-surface structures and/or the effect of cultural features (Roest et al., 1992). For the DC of the RTE_Inv grid, its usage led to the delineation of short wavelength magnetic anomalies up to a depth of 100 m from the Earth's surface. The process was vital in the optimization of the magnetic response of formations and structures in the top 100 m of the crust, where groundwater reserves are concentrated. Because the shortest wavelengths and data noise are amplified exponentially, the DC was employed with extreme caution (Reeves, 1989). All these aforementioned processing procedures were carried out using the Geosoft Oasis Montaj software.

Delineation of structures and structural complexity analysis

Variations in the crystalline basement and volcanic debris are the primary causes of magnetic anomalies. Sediments

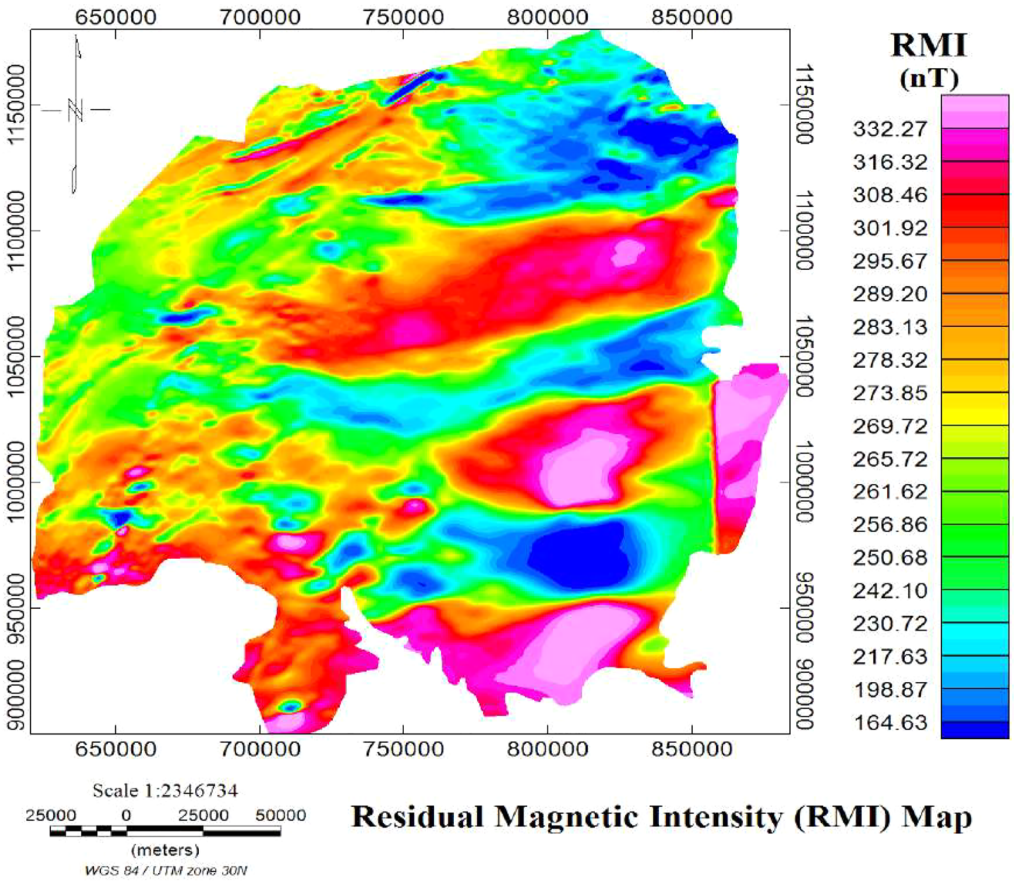

FIGURE 3 Map of the residual magnetic intensity .

are often magnetically "transparent," implying that their susceptibility is negligible. As a result, interpreting magnetic data can be a useful tool for investigating and analysing a basin's deepest and most fundamental geological structures. According to Kheyrollahi et al. (2016), one of the most important goals of the use of magnetic data is the delineation of geological formations and structures. Generally, groundwater accumulation, flow and storage in the Voltaian basin are largely controlled by the geological structures such as fracture zones along bedding planes for some areas. This is due to the fact that the primary porosity of these rocks is destroyed through consolidation and cementation. The geology, on the other hand, is based on the bedrock lithology as well as the regolith. The regolith is reported to be unsaturated in many areas and would thus only provide minor amounts of groundwater locally (Acheampong & Hess, 1998). In order to outline the structural network of the area, the first vertical derivative filter was employed on the RTE_Inv grid to delineate various lineaments.

The CET (Center of Exploration Targeting) grid analysis technique in Geosoft Oasis Montaj was applied to the downwardly continued and upwardly continued RTE_Inv grids to obtain structural lineaments up to 100 and 300 m, respectively. In carrying out this CET grid analysis technique, (1) each of the continued RTE_Inv grids was textually analysed to compute the local variations within the magnetic responses observed at each continued level; (2) various lineations (linear features) were identified based on the phase symmetry approach; (3) amplitude thresholding was carried out to find ridges, followed by line thinning (skeletonization) procedure and then vectorizing the skeletonized structures (thinned lines) to generate a vector lineament data (shown in Figure 7a) that would subsequently serve as input for the generation of the structural density heat map, otherwise known as the structural density map (Holden et al., 2012).

Evaluation and validation of structural density models

In this study, the structural density models generated for depth ranges 0–100 m and 100–300 m were evaluated and validated using the frequency ratio approach and the receiver operating characteristics (ROC) technique. The frequency ratio (FR) is a bivariate geostatistical approach that determines the spatial correlation of various classes of a geospatial model with respect to known locations of natural resource occurrence over a region of study. Thus, the aforementioned approach has proven worthy in determining the spatial association of various geospatial models with respect to known locations

of occurrences such as groundwater (P. O. Amponsah et al., 2023), mineral (P. O. Amponsah & Forson, 2023; Ghezelbash et al., 2021), flooding (Forson, Amponsah, et al., 2023; Forson & Menyeh, 2023), hydrocarbon (Arab Amiri et al., 2015) and landslide (Vakhshoori & Zare, 2016). The FR score for a particular class i (FR_i) of the structural density model is mathematically expressed as shown in Equation (1).

$$\mathrm{FR}_i = \frac{F_{\mathrm{BH}}}{F_{\mathrm{DM}}} = \frac{\mathrm{BH}_i/\mathrm{BH}_T}{\mathrm{DM}_i/\mathrm{DM}_T}, \quad (1)$$

where F_{BH} in Equation (1) depicts the groundwater occurrences (borehole points) within the class i of the structural density model; F_{DM} is the areal frequency of class i within the structural density model; BH_i is the number of boreholes in class i of the structural density model generated; BH_T is the total number of boreholes over the study area; DM_i is the area of class i in a generated structural density model, and DM_T is the total area of the structural density produced.

For a selected class i, the FR value greater than 1 depicts a strong correlation between the selected class and known locations of groundwater occurrence (borehole points) whereas an FR value less than 1 indicates that the selected class is weakly associated with the known locations of groundwater occurrences (borehole points).

The structural density models obtained for each depth range (0–100 m and 100–300 m) were further evaluated by overlaying borehole data with depths within their respective levels onto the structural density map (at depths 100 and 300 m) to determine the relationship between highly fractured zones and available borehole data. The efficacy of the relationship between the delineated structural density and borehole data was validated using the area under the receiver operating characteristics (ROC-AUC) curve. Area under the ROC values range from 0.5 to 1, with values close to 1 indicating outstanding performance and values close to 0.5 indicating poor prediction accuracy (P. O. Amponsah et al., 2023).

RESULTS

First vertical derivative map

Figure 4 depicts the first vertical derivative (1VD) of the magnetic responses within the study area. An essential component of the use of the 1VD technique is that it has the capacity to enhance anomalies associated with various structural features over a region of interest (Forson et al., 2021). In view of this, the generation of the 1VD map over the study area was vital in the delineation of various geological structures over the study area with the northern, mid-western and southern clusters as highly fractured.

From Figure 4, the central and eastern portions of the study area were, however, delineated to be poorly fractured. However, the northern, western and southwestern parts of the study area were delineated to be highly fractured. These clusters of geological structures among other factors play a major role in the groundwater dynamics of these areas. Hence, the delineated geological structural network (lineaments) acts as underground water channels (conduits for groundwater occurrence). This fault network has the potential to turn rocks into excellent aquifers. Again, faults act as drains, which influence the water level and thus affect groundwater distribution over an area of interest (Mulwa et al., 2009).

General structural characteristics (complexity) of the study area

Figure 5 characterizes various lineaments delineated by employing the Center of Exploration Targeting (CET) grid analysis technique on the RTE_Inv (shown in Figure 3b) over the study area. These lineaments depict aquifer fractures that are capable of enhancing the permeability and porosity within the area. Thus, lineaments to a great extent influence the occurrence and storage of groundwater within areas of their occurrence. The nature of the fractures can be an important factor in the morphology of the fractures (Acheampong & Hess, 1998). The different colouration observed from the legend of Figure 5a) depicts the trending directions of the delineated structures over the study area. In view of this, eastern trending structures have been indicated by deep green colouration whereas the structures which trend in the northern direction are represented by light green colours. North-western trending structures are depicted by blue colouration. Southern trending structures are shown in brown colours, and south-eastern trending structures are indicated in pink colours. The rose diagram (Figure 5b) shows the trend of lineaments in the study area. It is observed that the majority of the lineaments delineated within the study trend in the eastern direction. A substantial amount of the delineated structures also trend in the north-eastern and south-eastern directions. The area is dominated by eastern trending structures with a population of 1493 (50.61%). Dense regions of structural lineaments are essential to groundwater delineation because they depict low-pressure zones where fluids such as groundwater can settle (Forson et al., 2020; Forson, Wemegah, et al., 2022). The occurrence of structures within the Voltaian basin as established in the literature is a good indicator of potential groundwater zones since groundwater movement and storage are largely dependent on the structures in the area (Yidana et al., 2019). Figure 6 depicts the structural density over the study area and outlines highly, moderately and lowly fractured zones represented in red, green and blue colours, respectively. From Figure 6, the northern and the western parts of the study area were generally delineated as highly dense in terms of fracturing. Within the northern and

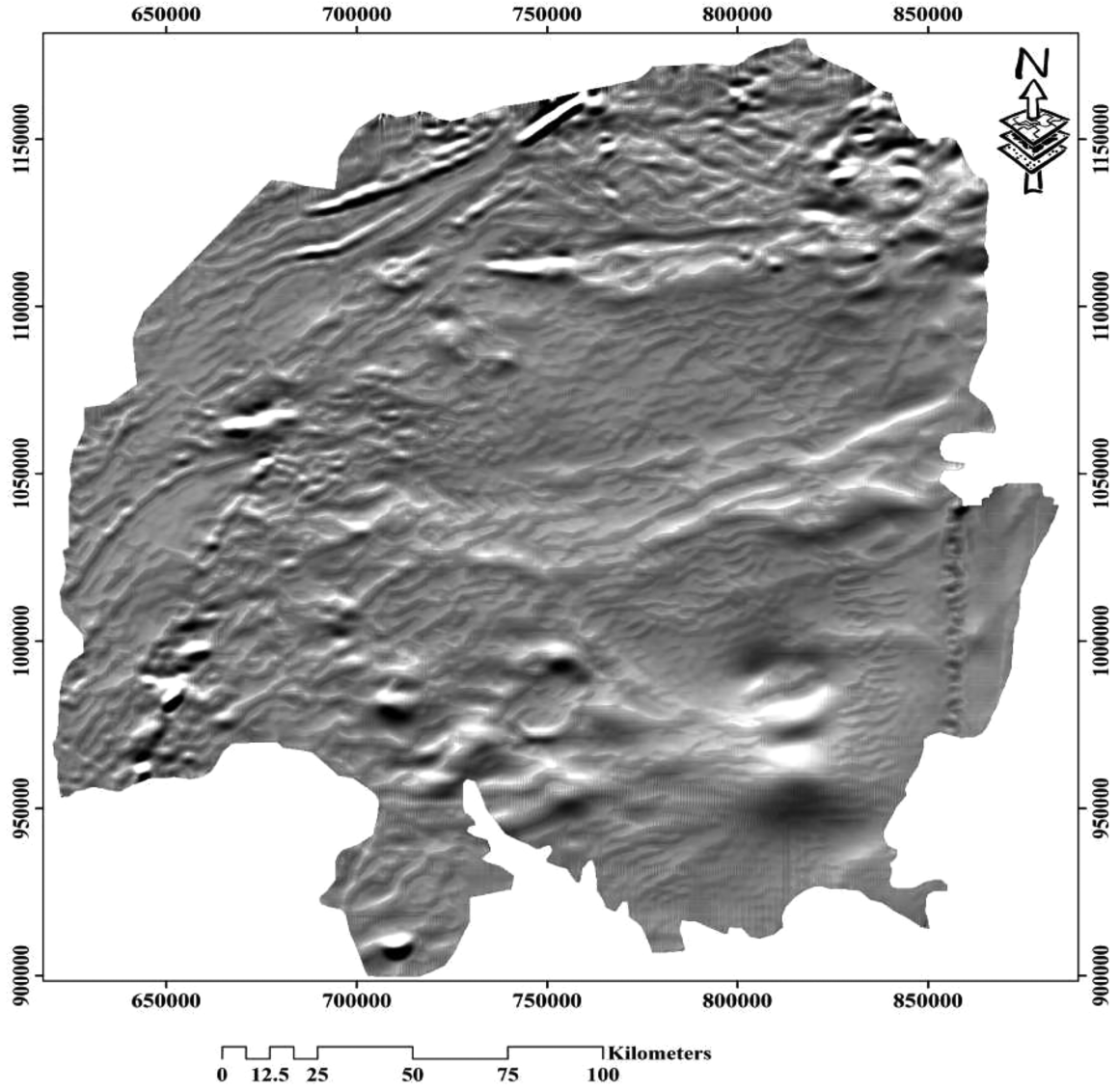

FIGURE 4 Qualitative image depicting responses generated based on the first vertical derivative of the magnetic field in a grey scale.

western regions, are characterised by acronyms comprising AN, OB, PA and CH which are dominantly composed of sandstone formation as well as BM, which is predominantly made up of mudstones. The area marked as BY, which is dominated by sandstones, was also delineated to be moderate to low dense zones in terms of structures. Groundwater availability is more likely to be plausible in areas with high structural density, whereas regions with low structural densities generally depict regions of low groundwater availability (Carney et al., 2010).

Structural complexity analysis from the Earth's surface to 100 m and from 100 m to 300 m over the study area

Producible depth ranges for groundwater exploration in Ghana especially within the northern sector of Ghana are mostly within the first 100 m beneath the Earth's surface with a few boreholes going beyond the 100-m depth (Agyekum & Asare, 2016; Manu et al., 2019). Various groundwater explorers rely on drilling outcomes within these shallow depth ranges (0–100 m) to assess the groundwater prospects of the Voltaian basin. It is worth noting that the capacity of the fracture dynamics (structural occurrences) at deeper depths within the basin has been rarely assessed in the literature (Carrier et al., 2008). In view of this, an understanding of the groundwater-producible zones of this basin requires knowledge of the depth of occurrence of geological structures in the basin. Figures 7a and 7b represents the delineated structural lineaments at depths 100 and 300 m, respectively. The minimum length of the delineated geological structures at the 100-m depth is 565.685 m (0.5657 km), whereas the maximum length of structures delineated at the same depth is 26,273.942 m (26.274 km). Up to a depth of 100 m, the total length of delineated geological

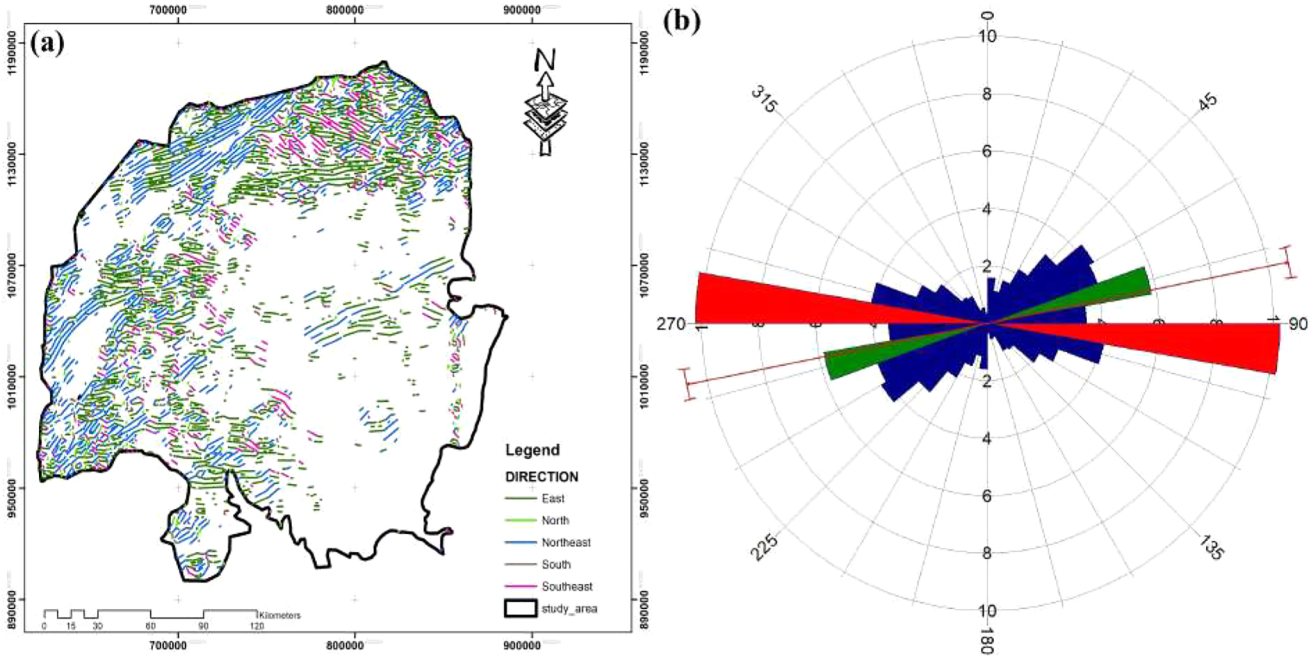

FIGURE 5 (a) Generalized structural complexity of the study area; (b) rose diagram depicting the trending direction of variously delineated structures within the study area.

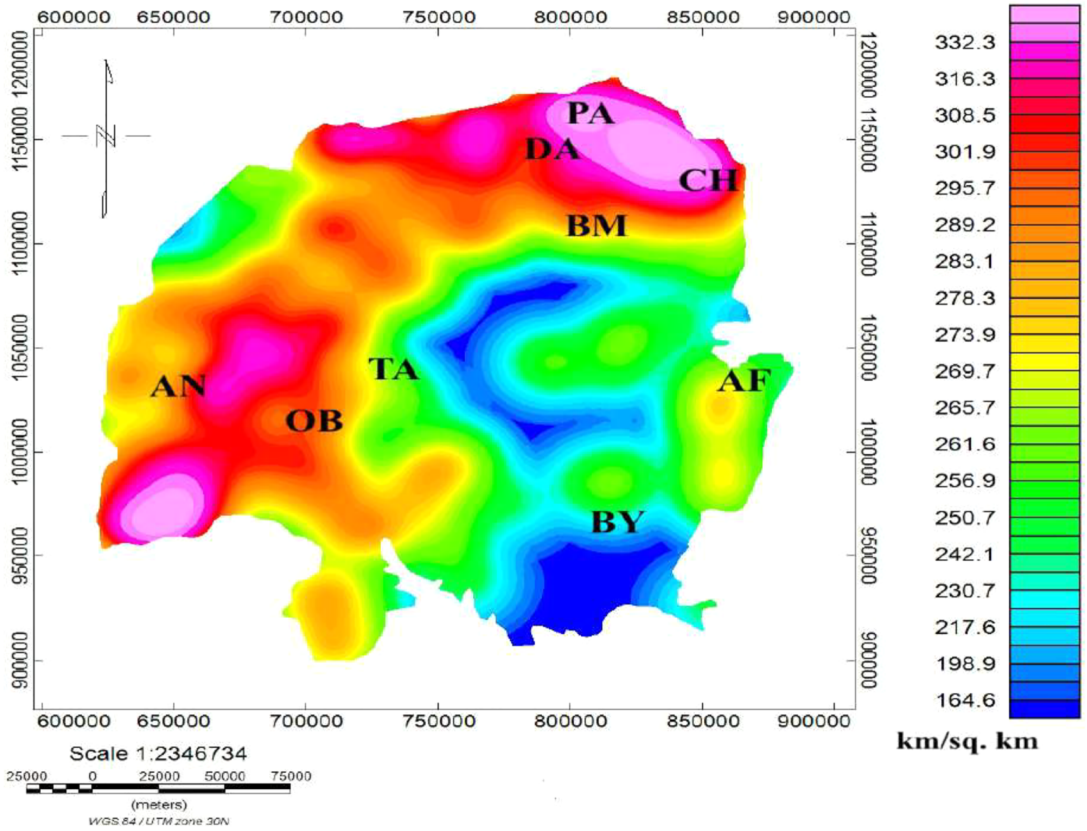

FIGURE 6 Generalized structural density map over the Voltaian basin.

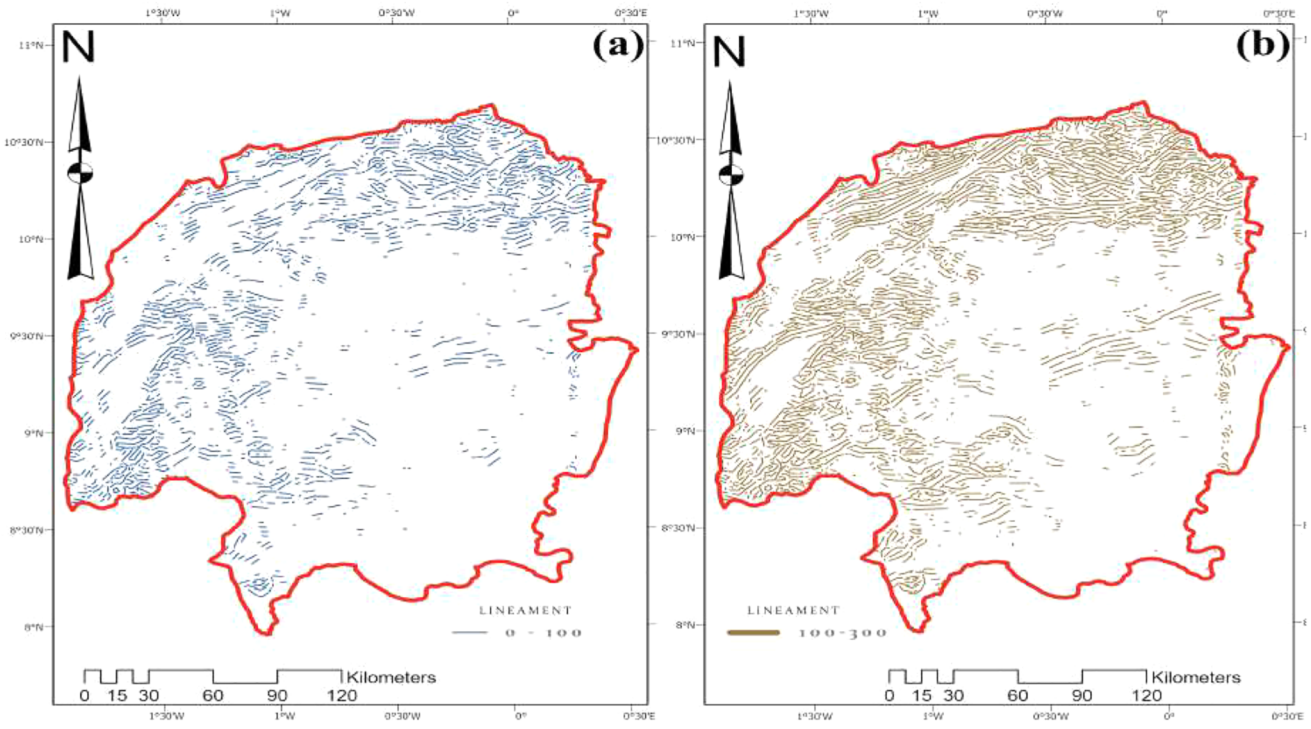

FIGURE 7 Delineated structures up to a depth of (a) 100 m and (b) 300 m within the Earth.

structures was 5,555,172.063 m (5555.172 km). The map (shown in Figure 7a) shows the northern portions to be more fractured, while the central and south-eastern portions are less fractured based on the structures delineated within the first 100 m of the Earth's surface. For depths up to 300 m within the Earth, the minimum and maximum lengths of all the geological structures delineated were, respectively, 447.2 and 27,103.5 m. The total length of geological structures outlined at the 300-m depth was 8,645,461 m. The map (shown in Figure 7b) shows several lineaments delineated over the northern, western and southwestern parts of the study area. This indicates the occurrence of intense fracturing within those regions. Although the central portions and south-eastern portions are less fractured in terms of the 300-m depth-delineated lineaments (Figure 7b), the few delineated structures in these areas are more dense and prominent than those delineated within the same zones observed on the 100-m depth structural map (shown in Figure 7a). In general, the delineated structures at the 300-m depth are more dense and longer than those delineated at the 100-m depth. The implication of this comparison, therefore, asserts that the lineaments or structures delineated at a depth of 300 m are more plausible for delineating groundwater within the study area than at a depth of 100 m since areas of intense fracturing (densely populated structures) depict low-pressure zones viable for hosting fluids including water (Forson et al., 2020; Nsiah et al., 2018).

The structural density models shown in Figure 8a,b characterize regions of high, moderate and low structural complexities (depicted as red, green and blue) observed at depths 100 m and 300 m over the study area. It can be observed that regions which were delineated to be predominant with the delineated structures (shown in Figure 7a,b) were also delineated to be highly dense in terms of structures on the structural density maps (Figure 8a and b). The range of structural density values obtained for various structures delineated up to a depth of 100 m was from 0 (very low structural density zones) to 110.9 km/km^2 (high structural density zones). These highly dense or intense regions of structural occurrences characterize highly fractured zones and are generally expected that groundwater potential in these areas would be significantly higher (Preeja et al., 2011). For the structures delineated at a depth of 300 m, the value of the density or intensity of various structures delineated ranged from 0 for very low-intensity regions to 158.1 km/km^2 for regions of high structural density. It can be observed that regions delineated to be characterized by moderate-to-high structural density occurrence at the 300-m derived SDM (Figure 8b) were more than that observed on the 100-m derived SDM (Figure 8a). Since high structural density zones depict favourable zones of groundwater occurrence, it, therefore, suggests that groundwater prospects are higher at deeper depths (up to a depth of 300 m) than in the shallower depths (up to a depth of 100 m) (Srivastava & Bhattacharya, 2006).

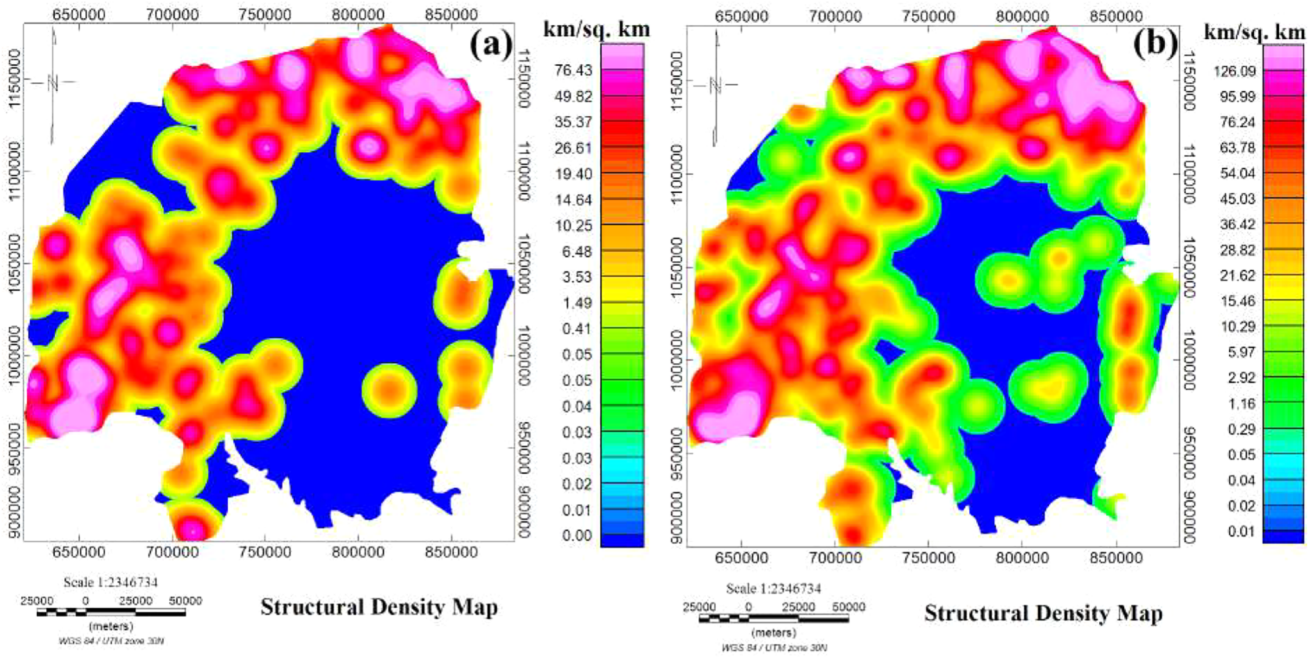

FIGURE 8 Structural density model up to a depth of (a) 100 m and (b) 300 m within the Earth.

TABLE 2 Discretized classes of structural density models and borehole yields (groundwater occurrences).

	Class description	SDM class values (km/km^2)	Classes of borehole yields (m^3/s)	Class score
100-m depth-derived SDM	Very low	≤31.0	≤10.0	1
	Low	31.1–59.9	10.1–40.0	2
	Moderate	60.0–80.0	40.1–150.0	3
	Moderately high	80.1–100.0	150.1–500.0	4
	Very high	>100.0	>500.0	5
300-m depth-derived SDM	Very low	≤32.0	≤10.0	1
	Low	32.1–62.0	10.1–40.0	2
	Moderate	62.1–95.0	40.1–150.0	3
	Moderately high	95.1–130.0	150.1–500.0	4
	Very high	>130.0	>500.0	5

Abbreviation: SDM, Structural density model.

Evaluation of structural density models using the frequency ratio approach

In order to assess the spatial relationship between the SDM produced and groundwater occurrence locations within them, they were discretized into five classes of very low, low, moderate, moderately high and very high structural density zones based on the Jenks natural breaking classification technique (Forson, Amponsah, et al., 2023; Jenks, 1963). This was carried out by overlaying known locations of groundwater occurrences (borehole yields) on the SDM (shown in Figure 9a,b). The description of the discretization results is summarized in Table 2. The application of the frequency ratio technique was essential in determining the spatial association of each class of the SDM with respect to known locations of groundwater occurrences within it. A summary of the frequency ratio results obtained for each class of the two SDM generated is presented in Table 3. In the case of the SDM generated at a depth of 100 m, the very low SDM class shows a weak correlation with the groundwater occurrences within the model due to the 0.744 frequency ratio (FR) value (less than 1) obtained. Groundwater occurrences were observed to exhibit strong coherence with respect to the four other SDM classes, and thus the frequency ratio values obtained are all greater than 1 (shown in Table 3). However, the moderately high class of the 100-m depth-generated SDM exhibited

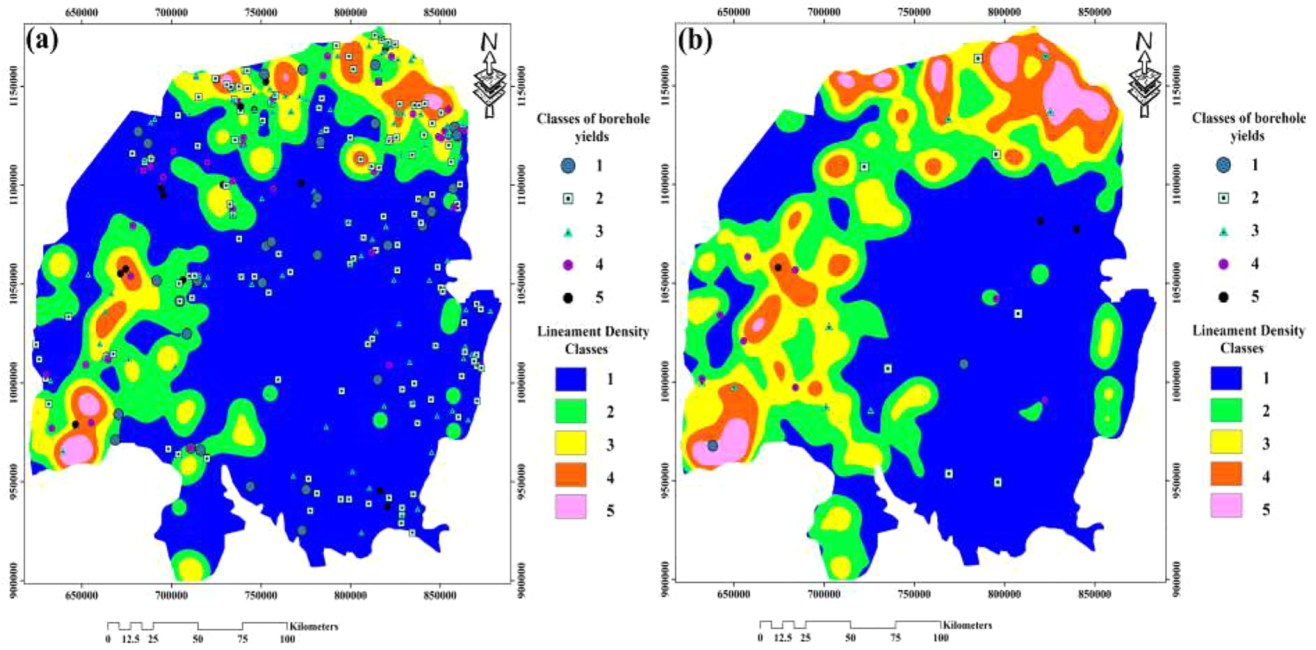

FIGURE 9 Discretized SDM derived (a) at 100 m and (b) at 300 m depth overlaid with corresponding known locations of groundwater.

TABLE 3 Frequency ratio values obtained for various classes within each of the two structural density models generated.

Structural density model (SDM)	Class	SDM class frequency (F_{DM})	Groundwater occurrence frequency (F_{BH})	Frequency ratio
	Very low	0.661	0.492	0.744
Up to a depth	Low	0.200	0.290	1.450
of 100 m	Moderate	0.093	0.140	1.505
	Moderately high	0.037	0.070	1.892
	Very high	0.008	0.009	1.125
	Very low	0.509	0.321	0.631
Up to a depth	Low	0.218	0.179	0.821
of 300 m	Moderate	0.1606	0.286	1.781
	Moderately high	0.081	0.143	1.765
	Very high	0.032	0.071	2.219

the strongest spatial relationship to groundwater occurrence. For the SDM produced for various lineaments delineated at a depth of 300 m within the Earth, the very low and low SDM classes were observed to show a weak association with groundwater occurrence with FR values of 0.631 and 0.821, respectively. The moderate, moderately high and very high classes of the 300-m depth-generated SDM exhibited a strong correlation to groundwater occurrences within the study area at that depth with FR values of 1.781, 1.765 and 2.219, respectively. In both structural density models, classes of high structural density were observed to have frequency ratio values greater than 1. This further indicates that groundwater occurrence or prospect within the study area is strongly associated with regions of high structural density. The frequency ratio results obtained, therefore, corroborate with the literature that groundwater prospects within the Voltaian basin are associated with fractured zones (structurally dense regions) (Loh et al., 2020). However, the high structural density class within the 300-m depth-derived SDM was observed to be the class with the strongest association with groundwater occurrence among all the classes within the two SDM-generated (SDM at 100 m and 300 m) data.

Validation of structural density models using the receiver operating characteristics curve

The spatial correlation between classes of SDM models and borehole yields (known locations of groundwater occurrence) was further assessed and validated using the receiver operating characteristics (ROC) technique. For the 100-m depth-derived SDM, an ROC output (shown in Figure 10) was

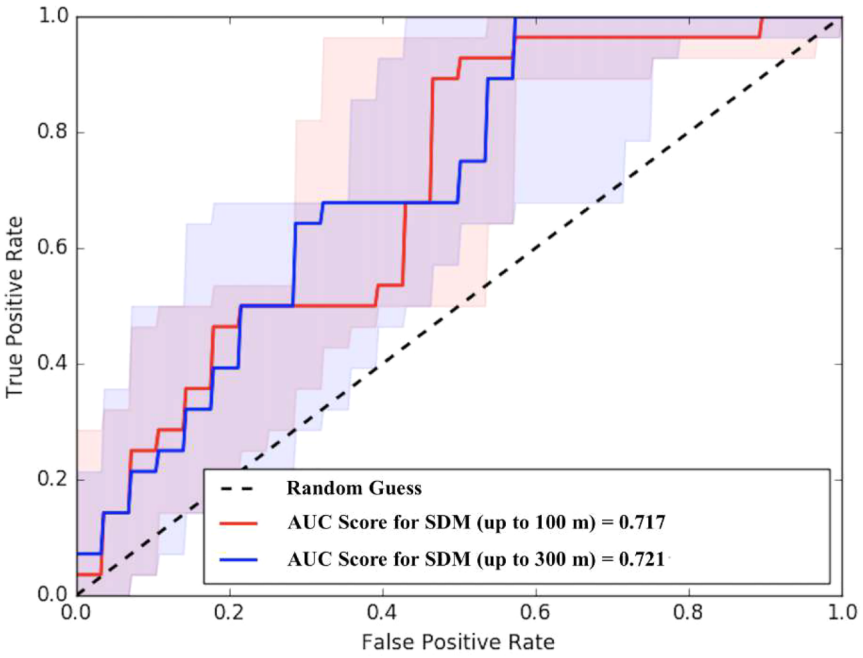

FIGURE 10 Area under the ROC curve score for the SDM at 100 m and 300 m.

produced by employing 378 operational boreholes with yields ranging from below 10 to above 500 m^3/s as validation point data. Thirty eight (38) operational boreholes were used for validating the 300-m depth-derived SDM based on the ROC results also shown in Figure 10. The outputs generated for the ROC were produced by discretizing the borehole yields into five classes depicting very low, low, moderate, moderately high and very high yields of groundwater as shown in Table 2. The score obtained for the area under the ROC curve (Area under the ROC [AUC]) for SDM derived at a depth of 100 and 300 m was, respectively, 0.715 (71.5%) and 0.721 (72.1%). The AUC score obtained (both of which are greater than 0.7) for each of the structural density models indicates that the models are efficiently produced. Nevertheless, comparing the AUC score obtained for the 100-m depth-derived SDM derived to the 300-m depth-derived SDM indicates a more efficient correlation between various classes of groundwater occurrence with respect to classes of SDM at a depth of 300 m (i.e., SDM derived at 300 m is more efficient than the SDM derived at a depth of 100 m).

CONCLUSION

In order to examine the relationship between groundwater occurrences and geological structures over the Voltaian basin, this study was carried out to delineate the density of various geological structures (structural density models) at a depth of 100 m and 300 m over the study area using the continuation techniques and the Centre of Exploration Targeting grid analysis technique. The structural density models (SDM) generated at a depth of 100 m and 300 m were evaluated to ascertain their spatial association with respect to the known locations of groundwater occurrences (borehole yields) using the frequency ratio technique. The frequency ratio results obtained for low structural density classes indicate a weak correlation with respect to the groundwater occurrences whereas the high structural density classes exhibited strong spatial association with respect to the known locations of groundwater occurrences. The frequency ratio results therefore corroborate with the literature that groundwater prospects within the Voltaian basin are associated with fractured zones (structurally dense regions). To further evaluate and validate the structural density models with respect to groundwater occurrences, the area under the receiver operating characteristics (ROC) technique was employed. Results obtained based on the ROC curve generated for the SDM derived at a depth of 100 m and 300 m were, respectively, 0.715 and 0.721. Although the efficacy of the two SDM-generated data was deemed very good (since ROC scores are greater than 0.7), the SDM derived at a depth of 300 m was observed to have a better performance than the SDM derived at a depth of 100 m.

ACKNOWLEDGEMENTS

The authors wish to thank the Ghana Geological Survey Authority, Accra, and the Community Water and Sanitation Agency of the Northern Region of Ghana for making the data available. Many thanks to the University of Ghana–Carnegie Corporation and the Building a New Generation Africa (BaNGA-Africa) for their immense support in making this study a success.

DATA AVAILABILITY STATEMENT

Data are available upon request to the corresponding author.

REFERENCES

Acheampong, S.Y. & Hess, J.W. (1998) Hydrogeologic and hydrochemical framework of the shallow groundwater system in the southern Voltaian Sedimentary Basin, Ghana. *Hydrogeology Journal*, 6(4), 527–537.

Agyekum, W. & Asare, E. (2016) Challenges associated with groundwater resources development in northern Ghana. *Ghana Journal of Science*, 56, 39–51.

Alhassan, S. & Hadwen, W.L. (2017) Challenges and opportunities for mainstreaming climate change adaptation into wash development planning in Ghana. *International Journal of Environmental Research and Public Health*, 14(7), 749.

Amponsah, P.O. & Forson, E.D. (2023) Geospatial modelling of mineral potential zones using data-driven based weighting factor and statistical index techniques. *Journal of African Earth Sciences*, 206, 105020.

Amponsah, P.O., Forson, E.D., Sungzie, P.S. & Loh, Y. S.A. (2023) Groundwater prospectivity modeling over the Akatsi districts in the Volta region of Ghana using the frequency ratio technique. *Modeling Earth Systems and Environment*, 9(2), 2081–2100.

Amponsah, T.Y., Danuor, S.K., Wemegah, D.D. & Forson, E.D. (2022) Groundwater potential characterisation over the Voltaian basin using geophysical, geological, hydrological and topographical datasets. *Journal of African Earth Sciences*, 192, 104558.

Annan-Yorke, R. & Cudjoe, J. (1971) *Geology of the Voltaian basin (summary of current ideas)*. Special Bulletin for Oil Exploration. *Geological Survey Department, Accra, Ghana*, 29.

Apambire, W.B. (2000) *Geochemical modeling and geomedical implications of fluoriferous groundwaters in the upper east region of Ghana*. University of Nevada, Reno.

Arab Amiri, M., Karimi, M. & Alimohammadi Sarab, A. (2015) Hydrocarbon resources potential mapping using evidential belief functions and frequency ratio approaches, southeastern Saskatchewan, Canada. *Canadian Journal of Earth Sciences*, 52(3), 182–195.

Blakely, R.J., Cox, A. & Iufer, E.J. (1973) Vector magnetic data for detecting short polarity intervals in marine magnetic profiles. *Journal of Geophysical Research*, 78(29), 6977–6983.

Carney, J.N., Jordan, C.J., Thomas, C.W., Condon, D.J., Kemp, S.J. & Duodo, J.A. (2010) Lithostratigraphy, sedimentation and evolution of the Volta basin in Ghana. *Precambrian Research*, 183(4), 701–724.

Carrier, M., Lefebvre, R., Racicot, J. & Asare, E. (2008) Northern Ghana hydrogeological assessment project. In *Access to sanitation and safe water—Global partnerships and local actions: Proceedings of the 33rd WEDC International Conference, Accra, Ghana*. Loughborough, UK: WEDC, Loughborough University, pp. 353–361.

Chegbeleh, L.P., Akudago, J.A., Nishigaki, M. & Edusei, S.N.K. (2009) Electromagnetic geophysical survey for groundwater exploration in the Voltaian of northern Ghana. *Journal of Environmental Hydrology*, 17, 1–16.

Darko, P.K. & Krásny, J. (2007) Regional transmissivity distribution and groundwater potential in hard rock of Ghana. In Krásný, J. & Sharp, J. M. (Eds) *Groundwater in fractured rocks*. IAH Selected Paper Series, volume 9. London: CRC Press, pp. 125–136.

Dzigbodi-Adjimah, K. (1993) Geology and geochemical patterns of the Birimian gold deposits, Ghana, West Africa. *Journal of Geochemical Exploration*, 47(1-3), 305–320.

Forson, E.D., Amponsah, P.O., Hagan, G.B. & Sapah, M.S. (2023) Frequency ratio-based flood vulnerability modeling over the Greater Accra Region of Ghana. *Modeling Earth Systems and Environment*, 9(2),2081–2100.

Forson, E.D. & Menyeh, A. (2023) Best worst method-based mineral prospectivity modeling over the Central part of the Southern Kibi–Winneba belt of Ghana. *Earth Science Informatics*, 16, 1657–1676.

Forson, E.D., Menyeh, A. & Wemegah, D.D. (2021) Mapping lithological units, structural lineaments and alteration zones in the Southern Kibi-Winneba belt of Ghana using integrated geophysical and remote sensing datasets. *Ore Geology Reviews*, 137, 104271.

Forson, E.D., Menyeh, A., Wemegah, D.D., Danuor, S.K., Adjovu, I. & Appiah, I. (2020) Mesothermal gold prospectivity mapping of the southern Kibi– Winneba belt of Ghana based on fuzzy analytical hierarchy process, concentration-area (CA) fractal model and prediction-area (PA) plot. *Journal of Applied Geophysics*, 174, 103971.

Forson, E.D., Wemegah, D.D., Hagan, G.B., Appiah, D., Addo-Wuver, F., Adjovu, I., Otchere, F.O., Mateso, S., Menyeh, A. & Amponsah, T. (2022) Data-driven multi-index overlay gold prospectivity mapping using geophysical and remote sensing datasets. *Journal of African Earth Sciences*, 190, 104504.

Ghezelbash, R., Maghsoudi, A., Bigdeli, A. & Carranza, E.J.M. (2021) Regional-scale mineral prospectivity mapping: support vector machines and an improved data-driven multi-criteria decision-making technique. *Natural Resources Research*, 30(3), 1977–2005.

Griffis, R., Barning, K., Agezo, F. & Akosah, F. (2002) *Gold deposits of Ghana*. Minerals Commission, Accra, Ghana, 432.

GSD (2010) *Geological map of Ghana*. Geological Survey Department.

Holden, E.-J., Wong, J.C., Kovesi, P., Wedge, D., Dentith, M. & Bagas, L. (2012) Identifying structural complexity in aeromagnetic data: an image analysis approach to greenfields gold exploration. *Ore Geology Reviews*, 46, 47–59.

Jenks, G.F. (1963) Generalization in statistical mapping. *Annals of the Association of American Geographers*, 53(1), 15–26.

Jordan, C., Carney, J., Thomas, C. & McDonnell, P. (2009) *Ghana airborne geophysics project in the Volta and Keta basins: BGS final report*. BGS commissioned report, CR/09/02. British Geological Survey.

Kheyrollahi, H., Alinia, F. & Ghods, A. (2016) Regional magnetic lithologies and structures as controls on porphyry copper deposits: evidence from Iran. *Exploration Geophysics*, 49(1), 98–110.

Kinnear, J.A., Binley, A., Duque, C. & Engesgaard, P.K. (2013) Using geophysics to map areas of potential groundwater discharge into Ringkøbing Fjord, Denmark. *The Leading Edge*, 32(7), 792–796.

Kortatsi, B. (1994) Groundwater utilization in Ghana. *IAHS Publications-Series of Proceedings and Reports-International Association of Hydrological Sciences*, 222, 149–156.

Loh, Y.S.A., Akurugu, B.A., Manu, E. & Aliou, A.-S. (2020) Assessment of groundwater quality and the main controls on its hydrochemistry in some Voltaian and basement aquifers, northern Ghana. *Groundwater for Sustainable Development*, 10, 100296.

MacDonald, A., Bonsor, H., Calow, R., Taylor, R., Lapworth, D., Maurice, L., Tucker, J. & O Dochartaigh, B. (2011) *Groundwater resilience to climate change in Africa*. British Geological Survey.

Mainoo, P.A., Manu, E., Yidana, S.M., Agyekum, W.A., Stigter, T., Duah, A.A. & Preko, K. (2019) Application of 2D-electrical resistivity tomography in delineating groundwater potential zones: case study from the Voltaian supergroup of Ghana. *Journal of African Earth Sciences*, 160, 103618.

Manu, E., Agyekum, W.A., Duah, A.A., Tagoe, R. & Preko, K. (2019) Application of vertical electrical sounding for groundwater exploration of Cape Coast municipality in the Central Region of Ghana. *Arabian Journal of Geosciences*, 12(6), 1–11.

Martin, N. & Van De Giesen, N. (2005) Spatial distribution of groundwater production and development potential in the Volta River basin of Ghana and Burkina Faso. *Water International*, 30(2), 239–249.

Mul, M., Obuobie, E., Appoh, R., Kankam-Yeboah, K., Bekoe-Obeng, E., Amisigo, B., Logah, F.Y., Ghansah, B. & McCartney, M. (2015) *Water resources assessment of the Volta River basin*. IWMI Working Paper 166. Colombo, Sri Lanka: International Water Management Institute.

Mulwa, J., Fairhead, D., Barongo, J. & Mariita, N. (2009) Heat source mapping and evaluation of geothermal resource potential in Lake Bogoria Basin, Kenya. In: *SEG Technical program expanded abstracts 2009*. Houston, TX: Society of Exploration Geophysicists, pp. 1294–1299.

Nabighian, M.N., Ander, M., Grauch, V., Hansen, R., LaFehr, T., Li, Y., Pearson, W., Peirce, J., Phillips, J. & Ruder, M. (2005) Historical development of the gravity method in exploration. *Geophysics*, 70(6), 63ND–89ND.

Nsiah, E., Appiah-Adjei, E.K. & Adjei, K.A. (2018) Hydrogeological delineation of groundwater potential zones in the Nabogo basin, Ghana. *Journal of African Earth Sciences*, 143, 1–9.

Nwachukwu, C., Orakwe, L. & Ogbu, K. (2018) Review of soil and water assessment tool (SWAT) application in sub-Saharan African countries. *Journal of Engineering and Applied Sciences*, 13, 1–10.

Obuobie, E., Barry, B. & Agyekum, W. (2016) Groundwater resources of the Volta basin. In: Williams, T.O., Mul, M., Biney, C.A., & Smakhtin, V. (Eds) *The Volta River basin: Water for food, economic growth and environment*. London: Routledge, pp. 66–81.

Preeja, K., Joseph, S., Thomas, J. & Vijith, H. (2011) Identification of groundwater potential zones of a tropical river basin (Kerala, India) using remote sensing and GIS techniques. *Journal of the Indian Society of Remote Sensing*, 39(1), 83–94.

Reeves, C. (1989) Aeromagnetic interpretation and rock magnetism. *First Break*, 7(7).

Roberts, N. (1982) A note on the geomorphological environment of Çatal Hüyük, Turkey. *Journal of Archaeological Science*, 9(4), 341–348.

Roest, W.R., Verhoef, J. & Pilkington, M. (1992) Magnetic interpretation using the 3-D analytic signal. *Geophysics*, 57(1), 116–125.

Sabins, F.F. (1999) Remote sensing for mineral exploration. *Ore Geology Reviews*, 14(3-4), 157–183.

Sankar, K. (2002) Evaluation of groundwater potential zones using remote sensing data in Upper Vaigai river basin, Tamil Nadu, India. *Journal of the Indian Society of Remote Sensing*, 30(3), 119–129.

Service, G.S. (2014) *2010 population and housing census report*. Accra: Ghana Statistical Service.

Smith, R.S., O'Connell, M.D. & Poulsen, L.H. (2004) Using airborne electromagnetics surveys to investigate the hydrogeology of an area near Nyborg, Denmark. *Near Surface Geophysics*, 2(3), 123–130.

Srivastava, P.K. & Bhattacharya, A.K. (2006) Groundwater assessment through an integrated approach using remote sensing, GIS and resistivity techniques: a case study from a hard rock terrain. *International Journal of Remote Sensing*, 27(20), 4599–4620.

Vakhshoori, V. & Zare, M. (2016) Landslide susceptibility mapping by comparing weight of evidence, fuzzy logic, and frequency ratio methods. *Geomatics, Natural Hazards and Risk*, 7(5), 1731–1752.

Yidana, S.M. (2010) Groundwater classification using multivariate statistical methods: Southern Ghana. *Journal of African Earth Sciences*, 57(5), 455–469.

Yidana, S.M., Vakpo, E.K., Sakyi, P.A., Chegbeleh, L.P. & Akabzaa, T.M. (2019) Groundwater–lakewater interactions: an evaluation of the impacts of climate change and increased abstractions on groundwater contribution to the Volta Lake, Ghana. *Environmental Earth Sciences*, 78(3), 74.

How to cite this article: Yaw Amponsah, T., Wemegah, D.D., Danuor, S.K. & Forson, E.D. (2023) Depth-based correlation analysis between the density of lineaments in the crystalline basement's weathered zones and groundwater occurrences within the Voltaian basin, Ghana. *Geophysical Prospecting*, 1–15. https://doi.org/10.1111/1365-2478.13422